Synthesis, Spectroscopy, Electrochemistry, Spectroelectrochemistry, Langmuir–Blodgett Film Formation, and Molecular Orbital Calculations of Planar Binuclear Phthalocyanines[1]

Nagao Kobayashi,*,†,2 Herman Lam,†,3 W. Andrew Nevin,†,4 Pavel Janda,†,5 Clifford C. Leznoff,*,† Toshiki Koyama,‡ Atsushi Monden,‡ and Hirofusa Shirai*,‡

Contribution from the Department of Chemistry, York University, North York (Toronto), Ontario, Canada M3J 1P3, and Department of Functional Polymer Science, Faculty of Textile Science and Technology, Shinshu University, Ueda 386, Japan

Received April 14, 1993®

Abstract: A planar binuclear phthalocyanine and its dizinc and dicobalt derivatives, in which two phthalocyanine units share a common benzene ring, have been studied by spectroscopy, electrochemistry, and spectroelectrochemistry. Their Langmuir–Blodgett film-forming properties have been examined, and the results of molecular orbital calculations on these and related systems are also presented. The properties are compared with those of the corresponding mononuclear control molecules. UV–visible–near IR absorption and magnetic circular dichroism spectroscopies and cyclic and differential pulse voltammetry indicate that, in these compounds, two relatively independent chromophore units interact and therefore that the two phthalocyanine planes are not completely planar in solution. The electrochemical and spectroelectrochemical measurements show the formations of various mixed-valence oxidation and reduction species in the binuclear compounds. The nonmetalated and dizinc complexes exhibit both S_1 and S_2 emission. The radiative lifetimes (τ) of the dizinc complex are smaller than those of the metal-free binuclear derivative for both S_1 and S_2 emission, while the quantum yields (ϕ_F) are larger. Furthermore, for S_2 emission, the ϕ_F and τ values of the binuclear compounds are larger than those of the corresponding mononuclear control molecules. Molecular orbital calculations within the framework of the Pariser–Parr–Pople approximation reproduce the splitting of the Q absorption band and further show that the splitting becomes larger the smaller the size of the shared common aromatic unit. In monolayers spread on water, the metal-free binuclear complex appears to have a slipped-stack conformation, tilted from the air–water interface normal plane. In Langmuir–Blodgett films, it may form a slipped-stack molecular arrangement with the stacking axis parallel to the substrate and/or a flat-lying conformation on the substrate surface.

Introduction

Phthalocyanines and porphyrins have recently been the subject of great interest in areas such as semiconductors,[6a,b] molecular metals,[6a,c] catalysis,[6d,e] and nonlinear optics.[6f,g] While the parent molecules have a number of useful properties, considerable effort has been made to synthesize novel structures, both with a view to engineering new molecular materials which may show improved or novel characteristics and to mimicking naturally occurring systems. In addition, much attention has focused on the formation of ordered thin-film assemblies, such as Langmuir–Blodgett (LB) films,[6h] which may be useful in applications such as molecular devices. In this respect, many porphyrin[7,8] and phthalocyanine[9–11] dimers[7,9,10] and oligomers[8,9a,c,11] and mixed porphyrin–phthalocyanine dimers[12] and multimers,[13] having various kinds of linkage, have been reported to date. These dimers and multimers, especially those with rigid cofacial configurations, often show spectroscopic and electrochemical properties which differ sig-

† York University.

‡ Shinshu University.

® Abstract published in *Advance ACS Abstracts,* December 15, 1993.

(1) Some preliminary results have been published: Leznoff, C. C.; Lam, H.; Marcuccio, S. M.; Nevin, W. A.; Janda, P.; Kobayashi, N.; Lever, A. B. P. *J. Chem. Soc., Chem. Commun.* **1987**, 699.

(2) Visiting professor from the Pharmaceutical Institute, Tohoku University, Sendai 980, Japan.

(3) Current address: Glaxo Canada Inc., 7333 Mississauga Road North, Mississauga, Ontario, Canada L5N 6L4.

(4) Current address: Central Research Laboratories, Kaneka Corporation, 2–80, 1-chome, Yoshida-cho, Hyogo-ku, Kobe 652, Japan.

(5) Visiting research associate from the Heyrovsky Institute of the Czech Academy of Sciences, Prague, Czechoslovakia.

(6) See, for example: (a) Simon, J; Andre, J.-J. *Molecular Semiconductors*; Springer: Berlin, 1985. (b) Nevin, W. A.; Chamberlain, G. A. *J. Appl. Phys.* **1991**, *69*, 4324. (c) Hoffman, B. M.; Ibers, J. A. *Acc. Chem. Res.* **1983**, *16*, 15. (d) Kobayashi, N.; Janda, P.; Lever, A. B. P. *Inorg. Chem.* **1992**, *31*, 5172. (e) Collman, J. P.; Zhang, X.; Lee. V. J.; Brauman, J. I. *J. Chem. Soc., Chem. Commun.* **1992**, 1647. (f) Rao, D. V. G. L. N.; Aranda, F. J.; Roach, J. F.; Remy, D. E. *Appl. Phys. Lett.* **1991**, *58*, 1241. (g) Norwood, R. A.; Sounik, J. R. *Appl. Phys. Lett.* **1992**, *60*, 295. (h) Snow, A. W.; Barger, W. R. In *Phthalocyanines—Properties and Applications*; Leznoff, C. C., Lever, A. B. P., Eds.; VCH Publishers: New York, 1989; Vol. 1, Chapter 5.

(7) There are many reports, but some representative papers are the following: (a) Collman, J. P.; Elliott, G. M.; Halbert, T. R.; Tovrog, B. S. *Proc. Natl. Acad. Sci. U.S.A.* **1977**, *74*, 18. (b) Kagan, N. E.; Mauzerall, D.; Merrifield, R. B. *J. Am. Chem. Soc.* **1977**, *99*, 5484. (c) Crossly, M. J.; Burn, P. L. *J. Chem. Soc., Chem. Commun.* **1987**, 39; **1991**, 1569. (d) Kobayashi, N.; Numao, M.; Kondo, R.; Nakajima, S.; Osa, T. *Inorg. Chem.* **1991**, *30*, 2241.

(8) (a) Migrom, L. R. *J. Chem. Soc., Perkin Trans. 1* **1983**, 2535. (b) Wennerstrom, O.; Ericsson, H.; Raston, I.; Svensson, S.; Pimlott, W. *Tetrahedron Lett.* **1989**, *30*, 1129.

(9) (a) Greenberg, S.; Marcuccio, S. M.; Leznoff, C. C.; Tomer, K. B. *Synthesis* **1986**, 406. (b) Nevin, W. A.; Hempstead, M. R.; Liu, W.; Leznoff, C. C.; Lever, A. B. P. *Inorg. Chem.* **1987**, *26*, 570. (c) Manivannan, V.; Nevin, W. A.; Leznoff, C. C.; Lever, A. B. P. *J. Coord. Chem.* **1988**, *19*, 139. (d) Kobayashi, N.; Lever, A. B. P. *J. Am. Chem. Soc.* **1987**, *109*, 7433. (e) Kobayashi, N.; Lam, H.; Nevin, W. A.; Janda, P.; Leznoff, C. C.; Lever, A. B. P. *Inorg. Chem.* **1990**, *29*, 3414. (f) Kobayashi, N. *J. Chem. Soc., Chem. Commun.* **1991**, 1203. (g) Levlievre, D.; Bosio, L.; Simon, J.; Andre, J.-J. *J. Am. Chem. Soc.* **1992**, *114*, 4475. (h) Kobayashi, N.; Yanagisawa, Y.; Osa, T.; Lam, H.; Leznoff, C. C. *Anal. Sci.* **1990**, *6*, 813.

(10) (a) Hush, N. S.; Woolsey, I. S. *Mol. Phys.* **1971**, *21*, 465. (b) Wheeler, B. L.; Nagasubramanian, G.; Bard, A. J.; Schechtman, L. A.; Dininny, D. R.; Kenney, M. E. *J. Am. Chem. Soc.* **1984**, *106*, 7404.

(11) (a) Nevin, W. A.; Liu, W.; Greenberg, S.; Hempstead, M. R.; Marcuccio, S. M.; Melnic, M.; Leznoff, C. C.; Lever, A. B. P. *Inorg. Chem.* **1987**, *26*, 891. (b) Simic-Glavaski, B.; Tanaka, A. A.; Kenney, M. E.; Yeager, E. *J. Electroanal. Chem.* **1987**, *229*, 285.

(12) (a) Gaspard, S.; Giaannotti, C.; Maillard, P.; Schaeffer, C.; Tran-Thi, T. H. *J. Chem. Soc., Chem. Commun.* **1984**, 856. (b) Tran-Thi, T. H.; Thiec, D. C.; Gaspard, S. *J. Phys. Chem.* **1989**, *93*, 1226.

(13) Kobayashi, N.; Nishiyama, Y.; Ohya, T.; Sato, M. *J. Chem. Soc., Chem. Commun.* **1987**, 390.

0002-7863/94/1516-0879$04.50/0

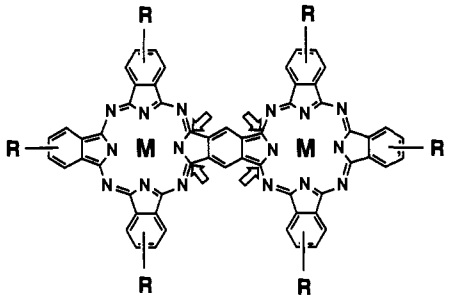

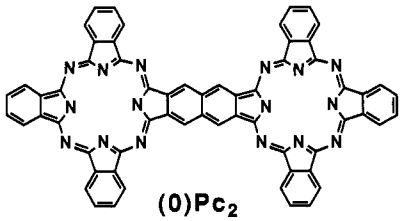

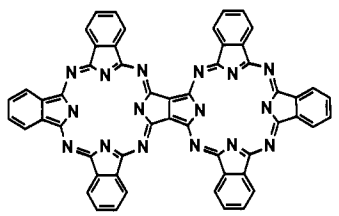

Figure 1. Planar binuclear phthalocyanines examined in this study and related macrocycles used for comparative molecular orbital calculations ((–1) in the abbreviation means that a benzene unit is lacking from the real dimer of phthalocyanine).

nificantly from the parent monomers. However, with the exception of a few brief reports,[1,7c,d,9f,g] no detailed study on the spectroscopy and electrochemistry of planar binuclear porphyrins and phthalocyanines has yet been carried out.

In this paper, we present the first detailed study on planar binuclear complexes among porphyrins and phthalocyanines. A systematic investigation of the spectroscopic, electrochemical, and spectroelectrochemical properties of a planar binuclear phthalocyanine, linked by a common benzene ring, and its dizinc and dicobalt derivatives (see Figure 1) has been carried out, augmented by theoretical molecular orbital calculations. As will be described below, the accumulated evidence indicates significant interaction between the two phthalocyanine chromophores. Surprisingly, the rings do not appear to lie completely flat, but may have a bent conformation in solution. In addition, the ability of the planar binuclear phthalocyanine to form monolayers and built-up multilayer LB films has been examined and compared with that of the corresponding mononuclear complex.

Experimental Section

(i) **Measurements.** Solvents for spectroscopic and electrochemical measurements, *N,N*-dimethylformamide (DMF) (Aldrich, Gold label, anhydrous, H_2O <0.005%, packed under nitrogen) and *o*-dichlorobenzene (DCB) (Aldrich, Gold label), were used as supplied. Spectrograde chloroform was distilled for Langmuir–Blodgett film formation. Tetrabutylammonium perchlorate (TBAP) (Kodak) was recrystallized from absolute ethanol and dried at 50 °C under vacuum for 2 days.

Measurements of electronic absorption, magnetic circular dichroism (MCD), fluorescence, excitation, and electron spin resonance (ESR) spectra were performed with equipment described in our previous papers.[7d,9b–e] Polarized absorption spectra were recorded using Jasco polarizers and changing the angle of the sample holder. Fluorescence quantum yields were determined by the use of quinine bisulfate in 1 N H_2SO_4 (ϕ_F = 0.55 at 296 K),[14a,b] free base tetraphenylporphyrin in benzene (ϕ_F = 0.11),[14c] or zinc phthalocyanine in 1-chloronaphthalene (ϕ_F = 0.30).[14c] Data were obtained by a comparative calibration method, using the same excitation wavelength and absorbance for the planar binuclear species and the calibrants and the same emission energies. Fluorescence decay curves were obtained at 20 °C by a Horiba NAES-550 series, using combinations of glass filters and solution filters of saturated $CuSO_4 \cdot 5H_2O$ aqueous solution and K_2CrO_4 (0.27 g/1000 mL of H_2O) and a monochromator for monitoring the emission. The lifetimes were determined from the decay curves by use of the least-squares method. All solutions for fluorescence measurements were purged with argon before measurement.

Cyclic (CV) and differential pulse voltammetry (DPV) were performed with a Princeton Applied Research (PARC) 174A polarographic analyzer coupled to a PARC 175 universal programmer. Electrochemical data were recorded under an atmosphere of nitrogen or argon, using a conventional three-electrode cell. A platinum disk described by the cross-sectional area of a 27-gauge wire (area 10^{-3} cm^2), sealed in glass, was used as the working electrode, and a platinum wire served as the counter electrode. The reference electrode was Ag/AgCl (0.045 V vs the saturated calomel electrode (SCE))[15] (in saturated KCl, separated by a frit), corrected for junction potentials by being referenced internally to the ferrocenium/ferrocene (Fc^+/Fc) couple. In various experiments involving DMF solutions, the Fc^+/Fc couple was seen to lie in the range +0.35 to +0.45 V vs Ag/AgCl/Cl^-, due to variations in junction potentials.[16] In DCB, the Fc^+/Fc couple was observed at approximately 0.59 V vs Ag/AgCl/Cl^-. All DMF solutions were prepared and measurements made under an atmosphere of nitrogen in a Vacuum Atmosphere Drilab. The DCB solutions were prepared in air, degassed by repeated freeze–pump–thaw cycles, and then transferred to the drybox. The stability of the Ag/AgCl/Cl^- electrode was checked using a solution of ferrocene in DCB; it was stable for at least 2 days. Spectroelectrochemical measurements were made with a 0.45 mm path-length optically transparent thin-layer electrode (OTTLE) cell, utilizing a gold minigrid (500 lines/in., 60% transmittance),[17] or with a 1 mm path-length OTTLE utilizing a Pt minigrid,[18] in conjunction with the Hitachi–Perkin–Elmer spectrometer. Solutions for electrochemistry and spectroelectrochemistry contained 0.1–0.3 M TBAP as supporting electrolyte.

The surface pressure vs area isotherms were studied using a commercial Langmuir trough (Kyowa FACE, 1999 cm^2), equipped with a film balance (Kyowa HBM-AP), at a compression rate of 16.7 cm^2 min^{-1}.

(ii) **Computational Method.** The (–1) binuclear phthalocyanine structure was constructed by using standard phthalocyanine X-ray structural data[19] and by making the rings perfectly planar and adopting D_{2h} symmetry. Molecular orbital (MO) calculations were performed for the tetraanion (deprotonated form) within the framework of the Pariser–Parr–Pople (PPP) approximation,[20] where the semiempirical parameters of Gouterman *et al.*[21a] were first chosen, but later a slightly different set of values which were recommended in a recent text[21b] was employed. The use of the latter parameters gave slightly better results; these are atomic valence state ionization potentials of 11.16 (carbon), 20.21 (central nitrogen), and 14.12 eV (imino nitrogen), together with atomic valence state electron affinities of 0.03 (carbon), 5.32 (central nitrogen), and

(14) (a) Melhuish, W. H. *J. Phys. Chem.* **1960**, *64*, 762. (b) Demas, J. N.; Crosby, G. A. *Ibid.* **1971**, *75*, 991. (c) Seybold, P. G.; Gouterman M. J. *J. Mol. Spectrosc.* **1969**, *31*, 1.

(15) Bard, A. J.; Faulkner, L. R. *Electrochemical Methods*; John Wiley: New York, 1980.

(16) The position of the ferrocene/ferrocenium couple is quite sensitive to the organic solvent employed: Gagne, R. R.; Koval, C. A.; Lisensky, D. C. *Inorg. Chem.* **1980**, *19*, 2854. Gritzner, G.; Kuta, J. *Electrochim. Acta* **1984**, *29*, 869; Bohling, D. A.; Evans, J. F.; Mann, K. R. *Inorg. Chem.* **1982**, *21*, 3546.

(17) Nevin, W. A.; Lever, A. B. P. *Anal. Chem.* **1988**, *60*, 727.

(18) Kobayashi, N.; Nishiyama, Y. *J. Phys. Chem.* **1985**, *89*, 1167.

(19) Robertson, J. M.; Woodward, I. *J. Chem. Soc.* **1937**, 219. Barrett, P. A.; Dent, C. E.; Linstead, R. P. *Ibid.* **1936**, 1719. Brown, C. J. *J. Chem. Soc. A* **1968**, 2488, 2494. Kirner, J. F.; Dow, W.; Scheidt, D. R. *Inorg. Chem.* **1976**, *15*, 1685.

(20) Pariser, R.; Parr, R. G. *J. Chem. Phys.* **1953**, *21*, 466, 767. Pople, J. A. *Trans. Faraday Soc.* **1953**, *46*, 1375.

(21) (a) Weiss, C.; Kobayashi, H.; Gouterman, M. *J. Mol. Spectrosc.* **1965**, *16*, 415. (b) Tokita, S.; Matsuoka, K.; Kogo, Y.; Kihara, K. *Molecular Design of Functional Dyes-PPP MO Method and Its Application*; Maruzen: Tokyo, 1990. (c) Hammond, H. *Theor. Chim. Acta* **1970**, *18*, 239. (d) Mataga, N.; Nishimoto, K. *Z. Phys. Chem. (Frankfurt am Main)* **1957**, *13*, 140.

Table 1. Electronic Absorption and MCD Data in DCB[a]

complex	electronic absorption λ/nm ($10^{-4}\epsilon/M^{-1}$ cm^{-1})				magnetic circular dichroism λ/nm ($10^{-5}[\theta]_M$/deg dm^3 mol^{-1} cm^{-1} T^{-1})				
ZnTNPc	349 (7.8)	616 (3.29)	684 (15.04)		334 (0.60)	360 (–0.88)	616 (4.21)	675 (19.05)	689 (–22.94)
(–1)[ZnTrNPc]$_2$	363 (7.27)	672 (5.77)	715 (7.46)	845 (1.42)	342 (0.26)	383 (–0.56)	638 (2.31)	667 (2.30)	706 (–3.36)
CoTNPc	433 (4.73)	615 (3.0)	681 (8.29)		349 (0.13)	380 (–0.38)	613 (2.57)	670 (4.77)	691 (–6.42)
(–1)]CoTrNPc]$_2$	362 (6.12)	675 (sh, 4.15)	713 (5.34)	864 (sh, 1.85)	339 (0.11)	396 (–0.42)		662 (1.72)	734 (–1.70)
H_2TNPc	347 (5.62)	672 (9.45)	709 (11.1)		333 (0.17)	357 (–0.27)	633 (1.42)	665 (2.17)	701 (–4.38)
(–1)[H_2TrNPc]$_2$	344 (7.08)	691 (7.94)	710 (7.59)		320 (0.28)	358 (–0.47)	624 (2.61)	683 (2.36)	701 (–5.08)

[a] Extinction coefficients of the binuclear compounds should be regarded as approximate, since they vary with the concentration of the solution for measurement due to a very high tendency toward aggregation.[1]

1.78 eV (imino nitrogen). Since the calculation was performed for (pyrrole proton-) deprotonated species, the central nitrogen atoms were assumed to be equivalent, supplying 1.5 electrons each to the π-system. In addition, σ polarizability was taken into account according to Hammond.[21c] Resonance integrals were taken to be –2.48 (β_{CN}) and –2.42 eV (β_{CC}).[21b] Two-center electron repulsion integrals were computed by the method of Mataga and Nishimoto.[21d] The choice of configurations was based on energetic considerations, and all singly excited configurations up to 56458 cm^{-1} were included. For comparison, MO calculations were also performed for the mononuclear phthalocyanine dianion with D_{4h} symmetry, and for tetraanions of planar binuclear phthalocyanines sharing none or two common benzene units, instead of a single benzene as in the (–1) phthalocyanines. These binuclear structures are also shown in Figure 1, together with their abbreviations.

(iii) **Langmuir–Blodgett and Nonorientated Film Formation.** The monolayer was spread on a triply distilled water subphase from a solution of tetraneopentoxyphthalocyanine (H_2TNPc, 1.12×10^{-5} M) or (–1)[H_2TrNPc]$_2$ (0.57×10^{-5} M) in chloroform at 10 °C. The built-up LB films of the Pc complexes were deposited by transfer of the monolayers using the horizontal lifting method onto quartz glass plates ($6.0 \times 4.5 \times 0.1$ cm) which had been rendered hydrophobic by pretreatment with 1% octadecyltrichlorosilane in $CHCl_3/CCl_4/C_{12}H_{25}$ (2:3:20 (v/v/v)), at a surface pressure of 16 mN m^{-1} with a dipping rate of 5 mm min^{-1} in an X-type transfer. Nonorientated films, which were used as references in the measurement of polarized adsorption spectra, were prepared by spin-coating.

(iv) **Synthesis. Bis(1,3-diiminoisoindoline).** Technical grade 1,2,4,5-tetracyanobenzene purchased from Pfaltz and Bauer Inc. was first purified by column chromatography using silica gel and dichloromethane/ether (1:1 v/v) as eluant. The front yellow fraction was found to contain sulfur and was therefore discarded. The next slightly yellow fraction was collected and recrystallized from ethanol. Mp: 265 °C (lit.[22] mp 258 °C). IR (cm^{-1}): 3100, 2250 (CN), 1590, 1280, 920. ^{1}H NMR ($CDCl_3$) δ: 9.95 (s, 2H). Mass (*m/z*): 178 (M$^+$). Thus, purified tetracyanobenzene (170 mg, 0.96 mmol) was added to 15 mL of dry methanol containing 15 mg of sodium. Ammonia gas was bubbled into the solution for 30 min at room temperature, and the solid was collected by filtration, washed with methanol, and dried to give crude bis(1,3-diiminoisoindoline). The IR spectrum of this compound did not exhibit nitrile absorption observed for the starting nitrile at 2250 cm^{-1}.

Bis(7^2,12^2,17^2-trineopentoxytribenzo[*g,l,q*]-5,10,15,20-tetraazaporphyrino)[*b,e*]benzene, *i.e.* nonmetalated negative-linked planar binuclear phthalocyanine, (–1)[H_2TrNPc]$_2$. Crude 5-neopentoxy-1,3-diiminoisoindoline obtained from 5.70 g (26 mmol) of 5-neopentoxyphthalonitrile[9a,b] and bis(1,3-diiminoisoindoline) obtained from 170 mg (0.96 mmol) of 1,2,4,5-tetracyanobenzene were refluxed for 44 h in 2-(*N,N*-dimethylamino)ethanol (25 mL).[23] The reaction mixture was allowed to cool and then poured into 200 mL of water. The resulting mixture was filtered and washed with water until the filtrate became clear. The residue was washed again with methanol and then dried overnight in an oven at 60 °C to give 4.0 g of crude product. Flash chromatography on silica gel of this product using a 5-cm-diameter column and 1:1 (v/v) toluene/hexane as eluant gave 3.0 g of the mononuclear tetraneopentoxyphthalocyanine (H_2TNPc) in 54% yield. Further elution using toluene followed by 2-methoxyethanol/toluene (2:98 v/v) gave a fraction consisting largely of the binuclear (–1)[H_2TrNPc]$_2$. This binuclear fraction was further purified by gel-permeation chromatography (Bio-Beads SX-1, 200–400 mesh), eluting with tetrahydrofuran. The front running binuclear fraction was separated from the slow moving mononuclear fraction. Final purification of the binuclear phthalocyanine was achieved by vacuum liquid chromatography (VLC) using toluene as the eluting solvent followed by gradually increasing the 2-methoxyethanol/toluene ratio (1:100 to 5:100 v/v). The VLC removed the last traces of H_2TNPc and gave 196 mg of binuclear (–1)[H_2TrNPc]$_2$ in 12% yield as a dark shining solid. IR (cm^{-1}): 3280 (NH), 1615, 1105, 1015 (NH). ^{1}H NMR ($CDCl_3$, 300 MHz) δ: 6.4–8.0 (br, aromatic), 3.3–3.7 (br, OCH_2), 0–2.5 (br, $(CH_3)_3C$), –2 to –3 (br, N*H*). Mass (*m/z*): 1468 (M$^+$). Anal. Calcd for $C_{88}H_{90}N_{16}O_6$: C, 72.01; H, 6.18; N, 15.27. Found: C, 71.80; H, 6.29; N, 14.96.

(Bis(7^2,12^2,17^2-trineopentoxytribenzo[*g,l,q*]-5,10,15,20-tetraazaporphyrino)[*b,e*]benzene)dicobalt(II), *i.e.* dicobalt complex of (–1)[H_2TrNPc]$_2$, (–1)[CoTrNPc]$_2$. A mixture of 50.6 mg (0.034 mmol) of (–1)[H_2TrNPc]$_2$ and 60 mg (0.46 mmol) of anhydrous cobalt(II) chloride in 10 mL of a 1:4 (v/v) mixture of 2-methoxyethanol/toluene was heated to 120 °C for 20 h under an argon atmosphere. Flash chromatography of the crude reaction mixture on a 1-cm-diameter column packed with silica gel and eluted with 2-methoxyethanol/toluene (1:50 v/v) gave 34.6 mg of (–1)-[CoTrNPc]$_2$ in 63% yield as a dark blue shining solid. IR (cm^{-1}): 2950, 1610, 1240, 1100, 760. Mass (*m/z*): 1581 (M$^+$). Anal. Calcd for $C_{88}H_{86}N_{16}O_6Co_2$: C, 66.87; H, 5.48; N, 14.16; Co, 7.45. Found: C, 67.11; H, 6.02; N, 14.04; Co, 7.36.

(Bis(7^2,12^2,17^2-trineopentoxytribenzo[*g,l,q*]-5,10,15,20-tetraazaporphyrino)[*b,e*]benzene)dizinc(II), *i.e.* dizinc complex of (–1)[H_2TrNPc]$_2$, (–1)[ZnTrNPc]$_2$. A mixture of 50 mg (0.034 mmol) of (–1)[H_2TrNPc]$_2$ and 100 mg (0.54 mmol) of anhydrous zinc acetate in 10 mL of a 1:4 (v/v) mixture of 2-methoxyethanol/toluene was heated to 120 °C for 22 h under argon. The crude mixture was chromatographed as described for (–1)[CoTrNPc]$_2$ to give 50 mg of (–1)[ZnTrNPc]$_2$ in 92% yield as a dark green solid. IR (cm^{-1}): 2960, 1620, 1100, 750. Mass (*m/z*): 1595 (M$^+$). Anal. Calcd for $C_{88}H_{86}N_{16}O_6Zn_2$: C, 66.22; H, 5.43; N, 14.05; Zn, 8.20. Found: C, 66.49; H, 5.62; N, 14.12; Zn, 8.28.

The electronic absorption and MCD data of the dimers are summarized in Table 1, together with those of the corresponding mononuclear control molecules.

Results and Discussion

(i) Electrochemistry. Figure 2 shows typical cyclic and/or differential pulse voltammograms (CV and DPV, respectively) of ZnTNPc and (–1)[ZnTrNPc]$_2$ in DMF or DCB, with values listed in Table 2. The data on mononuclear ZnTNPc have been reported recently;[9c,e] however, they are included here for comparison. (–1)[ZnTrNPc]$_2$ shows two oxidation and four reduction couples in DMF, corresponding in potential to one quasi-reversible one-electron oxidation and two quasi-reversible one-electron reductions of the phthalocyanine ring ($i_a = i_{c,i} \propto v^{1/2}$). From the amount of current in the cyclic voltammogram and/or the area of the peaks in the DPV voltammogram, the four reduction waves involve approximately one electron each, per binuclear molecule, although the charges in the first two reductions appear slightly larger than those in the third and fourth reductions. In oxidation, however, the charge under the first oxidation wave is significantly smaller than that under the second oxidation wave, although the summation of the two charges corresponds to two electrons per binuclear molecule. Similar results are seen in DCB solution. Thus, the stepwise oxidation and reduction data clearly indicate that the two phthalocyanine cores in (–1)[ZnTrNPc]$_2$ are interacting with each other. From the separation of the split waves, of *ca.* 250–340 mV, the energy of the interaction is about $(2.0–2.8) \times 10^{-3}$ cm^{-1}. These values are notably larger than for the oxidation of 1,8-naphthalene- or 1,8-anthracene- linked cofacially orientated dizinc complexes (Nap[ZnTrNPc]$_2$ or Ant-

(22) Lawton, E. A.; McRitchie, D. D. *J. Org. Chem.* **1959**, *24*, 26.
(23) Brach, P. J.; Ossanna, O. A.; Weinberger, L. *J. Heterocycl. Chem.* **1970**, *7*, 403.

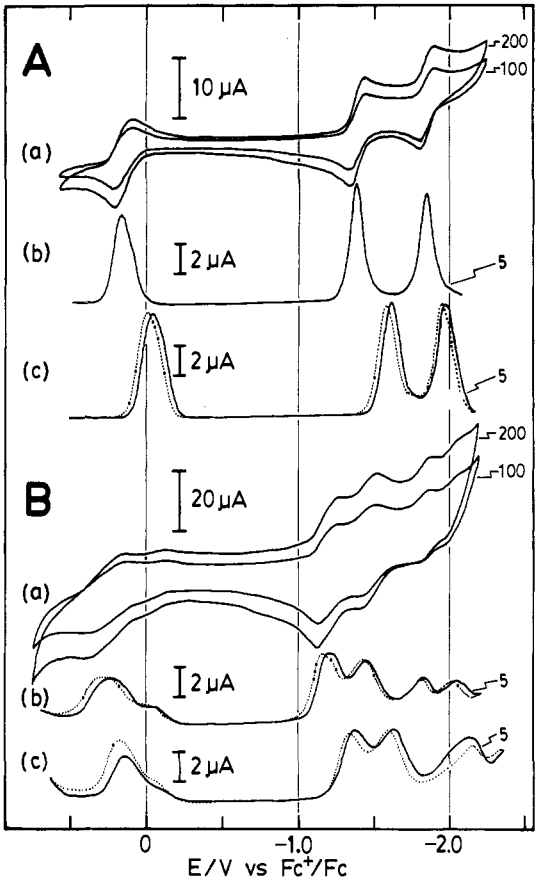

Figure 2. Cyclic and differential pulse (DP) voltammograms of (A) ZnTNPc and (B) (−1)[ZnTrNPc]$_2$ in DMF (curves a and b) and in DCB (curves c) at a Pt-disk working electrode. Numbers in the figures indicate sweep rate (in mV/s). In DP diagrams, solid lines indicate cathodic scan and dotted lines anodic scan. [ZnTNPc]/M = *ca.* 1×10^{-3} in DMF and 3×10^{-3} in DCB. [(−1)[ZnTrNPc]$_2$]/M = 6×10^{-4} in DMF and 2.95×10^{-4} in DCB. [TBAP]/M = 0.3.

[ZnTrNPc]$_2$, respectively), where the splitting of the first oxidation couple is *ca.* 210 mV (1.7×10^{-3} cm^{-1}).[9e] In addition, since the latter cofacial complexes do not show splitting of the reduction couples, the planar (−1)[ZnTrNPc]$_2$ complex is the first example of clear stepwise ring reduction in ring-linked binuclear phthalocyanines.

The separation between the averaged potentials of the first and second waves in the oxidation and reduction of (−1)-[ZnTrNPc]$_2$ is about 1.50 V, which is similar to the potential separation between the first oxidation and reduction couples in ZnTNPc. In comparison with mononuclear ZnTNPc, the first oxidation to the mixed-valence monocationic (−1)[ZnTrNPc-(−2)ZnTrNPc(−1)]$^+$ species is easier, while the second oxidation to (−1)[ZnTrNPc(−1)$^+$]$_2$ is harder than the oxidation of ZnTNPc-(−2) to ZnTNPc(−1)$^+$, *i.e.* the mononuclear oxidation couple lies approximately midway between the split waves of the binuclear oxidation couple. In contrast, on comparing the reduction processes of the planar binuclear and mononuclear zinc complexes, several interesting features appear. The first reduction step of the binuclear complex is shifted positively by about 300 mV, while the second reduction step occurs at a potential similar to that of the ZnTNPc(−2)/ZnTNPc(−3) couple. The third reduction potential of the binuclear complex is similar to that of the ZnTNPc(−3)/ZnTNPc(−4) couple, while the fourth potential occurs at a potential of about 200 mV further negative (see Figure 2 and Table 2). As a result, the separation between the averaged potentials of the first and second pairs of reduction waves of (−1)[ZnTrNPc]$_2$ is widened by about 200 mV compared to the potential separation of the first and second ring reductions of ZnTNPc. These phenomena may be due to the extended delocalization of the system, which lowers the energy of the molecular orbitals.

CV and DPV data were also measured for (−1)[CoTrNPc]$_2$ and are listed in Table 2, together with those of the mononuclear control molecule CoTNPc for comparison. Involvement of cobalt redox couples makes the response more complex than in the case of the zinc derivatives. In DCB, the splitting of the first ring-oxidation couple in (−1)[CoTrNPc]$_2$ becomes obscure, while that of the Co$^{II/I}$ couple is fairly large (*ca.* 500 mV), with a magnitude comparable to that in the 1,8-naphthalene- or 1,8-anthracene-linked cofacial binuclear phthalocyanines (390 and 480 mV, respectively).[9e] Although the summation of charges under these two split waves corresponds to nearly two electrons, the charge on the anodic side is much larger than that on the cathodic side. In particular, the ratio of charge (area) in the anodic scan of the differential pulse voltammogram is about 5:1. Thus, surprisingly, the reduction of the first cobalt atom of the binuclear complex appears to require a charge of more than one electron and that of the second cobalt less than one electron. The voltammetric responses in the ring-reduction region, between *ca.* −1.5 and −2.5 V, are complex. However, careful inspection indicates that four redox couples are involved. Since the total charge under these waves corresponds to approximately four electrons per binuclear molecule, the four couples are considered to imply a stepwise reduction of the two phthalocyanine units in (−1)[CoTrNPc]$_2$. This assignment is in agreement with the results of (−1)-[ZnTrNPc]$_2$, where the first ring-reduction couple is also shifted positively by more than 300 mV.

In contrast to the data in DCB, neither the Co$^{III/II}$ nor Co$^{II/I}$ redox couples of (-1)[CoTrNPc]$_2$ are split in DMF. This is also in contrast to the Nap- and Ant[ZnTrNPc]$_2$ cofacial systems, which show splitting of both the Co$^{III/II}$ and Co$^{II/I}$ couples in DMF.[9e] The different behavior may be related to axial coordination of DMF molecules to the cobalt atoms in the planar binuclear species, which may be sterically hindered in the cofacial complexes.

Table 3 lists comproportionation data for the zinc and cobalt (−1)[MtTrNPc]$_2$ complexes, obtained from the electrochemical data of Table 2. Comproportion constants (K_c at 20 °C) of the following mixed-valence formation reactions were calculated using eq 1, where ΔE is the splitting energy for the relevant split redox couple.

$$[MPc(-1)]_2 + [MPc(-2)]_2 \rightarrow 2[MPc(-1)MPc(-2)] \quad (I)$$

$$[MPc(-2)]_2 + [MPc(-3)]_2 \rightarrow 2[MPc(-2)MPc(-3)] \quad (II)$$

$$[MPc(-3)]_2 + [MPc(-4)]_2 \rightarrow 2[MPc(-3)MPc(-4)] \quad (III)$$

$$[Co^{II}Pc(-2)]_2 + [Co^{I}Pc(-2)]_2 \rightarrow 2[Co^{II}Pc(-2)Co^{I}Pc(-2)] \quad (IV)$$

$$\Delta E = (RT/F) \ln K_c \quad (1)$$

The K_c values lie approximately in the 2×10^2 to 1×10^8 range (ΔG = *ca.* −13 to −45 kJ mol^{-1}), indicative of significant delocalization in many of the species.[24] Table 3 also contains a comparison of literature data for Ant- and Nap[CoTrNPc]$_2$.[9e]

(ii) Spectroscopy. (a) Electronic Absorption and Magnetic Circular Dichroism Spectroscopy. Figure 3 shows the UV–visible–near-IR absorption and MCD spectra of (−1)[ZnTrNPc]$_2$ and the corresponding mononuclear ZnTNPc molecule in DCB

(24) (a) Gagne, R. R.; Spiro, C. L.; Smith, T. J.; Haman, C. A.; Thies, W. R.; Shiemke, A. K. *J. Am. Chem. Soc.* **1981**, *103*, 4073. (b) Sutton, J. E.; Taube, H. *Inorg. Chem.* **1981**, *20*, 319. (c) Suzuki, M.; Uehara, A.; Oshio, H.; Yanaga, M.; Kida, S.; Sato, K. *Bull. Chem. Soc. Jpn.* **1987**, *60*, 3547.

Table 2. Electrochemical Data for Mononuclear and Binuclear Zinc and Cobalt Derivatives

couple	DCB solution $E_{1/2}/V^a$	DMF solution $E_{1/2}/V^a$
	ZnTNPc system[b]	
Pc(−1)/Pc(−2)	−0.02	0.15
Pc(−2)/Pc(−3)	−1.66	−1.43
Pc(−3)/Pc(−4)	−2.04	−1.85
	(−1)[ZnTrNPc]$_2$ system	
[Pc(−1)]$_2$/[Pc(−1)Pc(−2)]	0.16	0.26
[Pc(−1)Pc(−2)]/[Pc(−2)]$_2$	−0.09	−0.08
[Pc(−2)]$_2$/[Pc(−2)Pc(−3)]	−1.35	−1.19
[Pc(−2)Pc(−3)]/[Pc(−3)]$_2$	−1.61	−1.44
[Pc(−3)]$_2$/[Pc(−3)Pc(−4)]	−1.95[c]	−1.83
[Pc(−3)Pc(−4)]/[Pc(−4)]$_2$	−2.20[c]	−2.04
	CoTNPc system[b]	
$Co^{III}Pc(-1)/Co^{II}Pc(-1)$	0.59	
$Co^{III}Pc(-1)/Co^{III}Pc(-2)$		0.38
$Co^{II}Pc(-1)/Co^{II}Pc(-2)$	0.03	
$Co^{III}Pc(-2)/Co^{II}Pc(-2)$		−0.02
$Co^{II}Pc(-2)/Co^{I}Pc(-2)$	−0.91	−0.85
$Co^{I}Pc(-2)/Co^{I}Pc(-3)$	−2.07	−1.99
	(−1)[CoTrNPc]$_2$ system	
$[Co^{III}Pc(-1)Co^{III}Pc(-2)]/[Co^{III}Pc(-2)]_2$		0.58
$[Co^{III}Pc(-1)Co^{II}Pc(-1)]/[Co^{II}Pc(-1)]_2$ or $[Co^{III}Pc(-1)]_2[Co^{II}Pc(-1)]_2$	0.63	
$[Co^{III}Pc(-2)]_2/[Co^{II}Pc(-2)]_2$		0.03
$[Co^{II}Pc(-1)]_2/[Co^{II}Pc(-2)]_2$	0.18	
$[Co^{II}Pc(-2)]_2/[Co^{I}Pc(-2)]_2$		−0.78
$[Co^{II}Pc(-2)]_2/[Co^{II}Pc(-2)Co^{I}Pc(-2)]$	−0.81	
$[Co^{I}Pc(-2)Co^{II}Pc(-2)]/[Co^{I}(Pc(-2)]_2$	−1.29	
$[Co^{I}Pc(-2)]_2/[Co^{I}Pc(-2)Co^{I}Pc(-3)]$	−1.69	−1.33
$[Co^{I}Pc(-2)Co^{I}Pc(-3)]/[Co^{I}Pc(-3)]_2$	−1.96	−1.60
$[Co^{I}Pc(-3)]_2/[Co^{I}Pc(-3)Co^{I}Pc(-4)]$	−2.04	−1.82
$[Co^{I}Pc(-3)Co^{I}Pc(-4)]/[Co^{I}Pc(-4)]_2$	−2.20	−1.95

[a] Potentials are reported with respect to the Fc^+/Fc couple. [b] Data from ref 9e. [c] Approximate values.

Table 3. Comproportionation Data

compound	couple[a]	solvent[b]	$\Delta E/V^c$	K_c^d	K_d^e	ΔG/kJ mol^{-1}
(−1)[ZnTrNPc]$_2$	I	DCB	0.25	2.0×10^4	5.0×10^{-5}	−24
	I	DMF	0.34	7.0×10^5	1.4×10^{-6}	−33
	II	DCB	0.26	3.0×10^4	3.4×10^{-5}	−25
	II	DMF	0.25	2.0×10^4	5.0×10^{-5}	−24
	III	DCB	0.25	2.0×10^4	5.0×10^{-5}	−24
	III	DMF	0.21	4.1×10^3	2.4×10^{-4}	−20
(−1)[CoTrNPc]$_2$	IV	DCB	0.48	1.8×10^8	5.6×10^{-9}	−46
	II	DCB	0.27	4.4×10^4	2.3×10^{-5}	−26
	II	DMF	0.27	4.4×10^4	2.3×10^{-5}	−26
	III	DCB	0.16	5.6×10^2	1.8×10^{-3}	−15
	III	DMF	0.13	1.7×10^2	5.8×10^{-3}	−13
Ant[CoTrNPc]$_2$[f]	IV	DCB	0.48	1.8×10^8	5.6×10^{-9}	−46
	IV	DMF	0.30	1.4×10^5	7.0×10^{-6}	−29
Nap[CoTrNPc]$_2$[f]	IV	DCB	0.39	4.0×10^6	2.5×10^{-7}	−38
	IV	DMF	0.22	6.1×10^3	1.7×10^{-4}	−21

[a] I–IV correspond to couples I–IV in the text. [b] DCB = *o*-dichlorobenzene; DMF = *N*,*N*-dimethylformamide. [c] Mixed-valence splitting energy. [d] Comproportionation constant. [e] Disproportionation constant, $1/K_c$. [f] Reference 9e.

solution with data for these and for the cobalt and metal-free derivatives listed in Table 1. Compared with the absorption spectra of the mononuclear MtTNPcs, those of binuclear phthalocyanines are broader and extend into the near-IR region. In addition, although the intensity of the main Q band of the mononuclear phthalocyanines is generally larger than that of the Soret band, in the (−1) binuclear complexes the intensities are almost comparable. An unusual additional absorption peak is commonly observed in the near-IR region for the (−1) species (see Table 1).

In order to facilitate the interpretation of these spectra, we will first examine the spectrum of (−1)[ZnTrNPc]$_2$ because of its relative simplicity. In this case, four bands are seen in the Q-band region. From the interpeak energy and intensity differences, the bands at 715 and 645 nm are considered to belong to one couple and those at 672 and 603 nm to a second couple. In each couple, the band at lower energy appears to correspond to the Q_{0-0} band, while that at higher energy may be the Q_{0-1} vibrational band. Compared with the position of the Q_{0-0} band of mononuclear ZnTNPc, the bands in (−1)[ZnTrNPc]$_2$ lie at both lower and higher energy; hence, the Q band of this binuclear compound is composed of a doublet. In (−1)[ZnTrNPc]$_2$, the Q band of each monomer unit arises from nearly degenerate excited states, X_1, Y_1 on one unit and X_2, Y_2 on the other. Although the exact interaction among the four excited states depends on the detailed geometry, to a first approximation the four states interact in pairs. Thus, the four resulting dimeric excited states are roughly of the form $(X_1 \pm X_2)(2)^{-1/2}$ and $(Y_1 \pm Y_2)(2)^{-1/2}$. The expected geometry would have the transition dipoles of one pair of states, say X_1 and X_2, parallel to the vector **R** between the centers; the allowed exciton state is then the one at lower energy. The transition dipoles for the other pair, *i.e.* Y_1 and Y_2, would be perpendicular to **R**, and the allowed exciton state may be unshifted or blue shifted. This accounts for the well-resolved doublet in the Q-band region. Some intensity difference in the doublet is an indication of the occurrence of a bent structure for the dimer

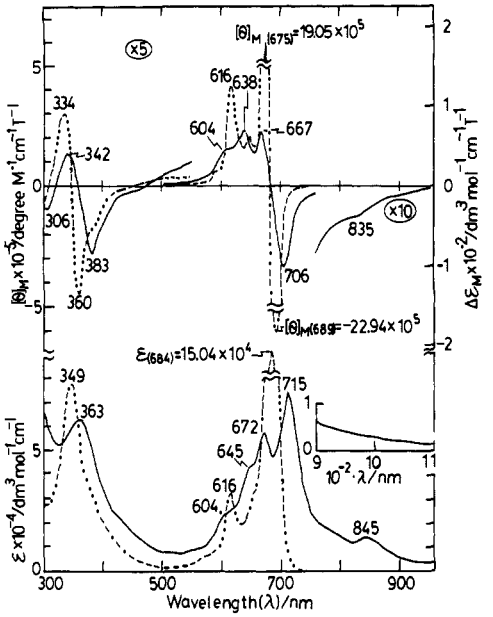

Figure 3. UV-visible absorption (bottom) and MCD (top) spectra of (−1)[ZnTrNPc]$_2$ and ZnTNPc in DCB. [(−1)[ZnTrNPc]$_2$]/M = 1.67 × 10^{-5}, [ZnTNPc]/M = 1.11 × 10^{-5}. Cell path length/mm = 10. The spectra of (−1)[ZnTrNPc]$_2$ derivatives are shown by solid lines and those of ZnTNPc by broken lines.

and/or a nonequality of X_1 (or X_2) and Y_1 (or Y_2) (in a mononuclear MtPc with D_{4h} symmetry, X_1=Y_1).[25] Since the occurrence of the near-IR band cannot be explained by coplanar interacting dipoles,[26] the two phthalocyanine units are considered to be tilted toward one another. Hence, these considerations, together with the results described in section i, indicate that the (−1) phthalocyanines are not flat in solution. From the Corey–Pauling–Koltun (CPK) molecular model, it is anticipated that the four positions shown in Figure 1 by arrows should be relatively flexible. Accordingly, if the (−1) phthalocyanines have a tilted conformation, the bending may occur at these positions.

The MCD spectra may be interpreted on a similar basis. Although we cannot distinguish from MCD whether the two phthalocyanine units in the (−1) phthalocyanines have a bent or twisted conformation, it is at least understandable that the Q-band MCD is composed of the superimposition of two *pseudo* Faraday *A* terms. As a result of the superimposition of two Faraday *A* terms at slightly different energies (*ca.* 900–1000 cm^{-1}), their intensity is much smaller than that of the mononuclear control molecule (Table 1). However, the *A*/*D* values (an MCD parameter) for the Q band, estimated by the method of Briat *et al.*,[27] do not differ greatly between the mononuclear and binuclear complexes (see Table 4). Similar behavior has been observed for a tetrabenzoporphyrin and its planar binuclear dimer[7d] and for crown-ether-substituted mononuclear Pcs and their cation-induced dimers.[28] A positive (negative in sign) *B* term was observed corresponding to the weak near-IR absorption band.

(b) Emission Spectroscopy. Figure 4 shows the fluorescence emission and excitation spectra of H_2TNPc, (−1)[H_2TrNPc]$_2$, and (−1)[ZnTrNPc]$_2$, and in Table 5 the obtained quantum yields (ϕ_F) and lifetimes (τ) are listed, together with those of ZnTNPc. All four compounds show so-called S_1 and S_2 emission, as has been found commonly for alkoxy group-substituted Pcs.[9d,29] In each case, the Stokes shift of the S_1 emission is very small, while that of the S_2 emission is generally large. The quantum yield of the S_1 emission of (−1)[H_2TrNPc]$_2$ is about 1 order of magnitude smaller than that of mononuclear H_2TNPc. This weak emission in the binuclear complex is an indication of intramolecular interaction between the two included units.[7b,25,30] In addition, the lifetime of the S_1 emission of (−1)[H_2TrNPc]$_2$ in deaerated chloroform is shorter than that of H_2TNPc, as has been observed previously in porphyrin systems.[25,30] The ϕ_F value of the S_1 emission of (−1)[ZnTrNPc]$_2$ is comparable to that of (−1)[H_2TrNPc]$_2$, but its lifetime is shorter.

Present knowledge on S_2 emission of phthalocyanines is still very limited.[9d,29,31] Ferraudi *et al.*[31] reported the first analysis of S_2 emission for aluminum and rhodium phthalocyanines in 1982, where the ϕ_F values were between 0.0012 and 0.0016 and the decay curves could be fitted by double-exponential functions. In the analysis of the broad S_2 emission of our compounds, some interesting features emerge (see Table 5). Firstly, as in ref 31, two components are required to obtain a relatively good fit of the decay curves, and the ratio of these two components does not differ greatly for both the mononuclear and binuclear complexes. Secondly, the obtained lifetimes for the binuclear complexes are always larger than those of the corresponding mononuclear compounds, indicating that the Soret excited state of the binuclear complexes is more stable. In addition, since τ values of 12–18 ns seem fairly large for states with a singlet multiplicity,[32] the S_2 emission may be originating in ligand-centered triplet states, such as π–π^*. Thirdly, contrary to the case of S_1 emission,[7d,30] the quantum yields of the zinc derivatives are much larger than those of the metal-free complexes for both the mononuclear and binuclear compounds, and in addition, the ϕ_F value of the binuclear complex is always larger than that of its mononuclear control molecule.

(iii) Spectroelectrochemistry. In order to observe the interaction between the halves of the molecules as a function of oxidation state and to confirm the assignment of the redox couples, spectroelectrochemical experiments were performed for (−1)[ZnTrNPc]$_2$ and (−1)[CoTrNPc]$_2$ complexes in solution. Figure 5A shows the two-step oxidation of (−1)[ZnTrNPc]$_2$ to its Zn^{II}–Zn^{II} ring-oxidized dication. As in the case of the formation of the monocation radical of ZnTNPc,[9c] both the Soret and main Q bands decrease in intensity, while the absorption in the region between the Soret and Q bands increases continuously. The stepwise nature of the oxidation process is shown by a reversal in the direction of the absorbance changes of the near-IR band at 845 and at *ca.* 1090 nm. If, as discussed in section ii, the near-IR band at 845 nm is an indication of the nonplanarity of the two included units, the oxidized species appear to be more planar than the neutral molecule, since the intensity of this band decreases upon oxidation.

Interpretation of the spectra of cation radical species of MtPcs has been attempted in several reports.[9c,33a–d] In the case of the ZnPc π-cation radical, the broad absorption near 500 nm has been attributed to a transition between nondegenerate states[33a] and a weak broad absorption at *ca.* 1000–1200 nm to a π–π^* transition rather than an intervalence transition.[9c] The π-cations of the lanthanide porphyrin[33e] or Pc[33d] complexes also show a near-IR band around 1100–1600 nm, which has been assigned

(25) Selensky, R.; Holten, D.; Windsor, M. W.; Paine, J. B., III; Dolphin, D.; Gouterman, M.; Thomas, J. C. *Chem. Phys.* **1981**, *60*, 33.
(26) Gouterman, M.; Holten, D.; Lieberman, E. *Chem. Phys.* **1977**, *25*, 139.
(27) Briat, B.; Schooley, D. A.; Records, R.; Bunnenberg, E.; Djerassi, C. *J. Am. Chem. Soc.* **1967**, *89*, 7062.
(28) Gasyna, Z.; Kobayashi, N.; Stillman, M. J. *J. Chem. Soc., Dalton Trans.* **1989**, 2397.
(29) Kobayashi, N.; Ashida, T.; Osa, T. *Chem. Lett.* **1992**, 2031.
(30) Kaizu, Y.; Maekawa, H.; Kobayashi, H. *J. Phys. Chem.* **1986**, *90*, 4234.
(31) Muralidharan, S.; Ferraudi, G.; Patterson L. K. *Inorg. Chim. Acta* **1982**, *65*, L235.
(32) Generally, subnanosecond lifetimes have been reported for the fluorescence of phthalocyanines: Menzel, E. R.; Rieckhoff, K. E.; Voigt, E. M. *Chem. Phys. Lett.* **1972**, *13*, 604. Brannon, J. H.; Magde, D. *J. Am. Chem. Soc.* **1980**, *102*, 62.
(33) (a) Nyokong, T.; Gasyna, Z.; Stillman, M. J. *Inorg. Chem.* **1987**, *26*, 548, 1087. (b) Homborg, H. *Z. Anorg. Allg. Chem.* **1983**, *507*, 35. (c) Homborg, H.; Teske, C. L. *Z. Anorg. Allg. Chem.* **1985**, *527*, 45. (d) Markovitsi, D.; Tran-Thi, T. H.; Even, R.; Simon, J. *Chem. Phys. Lett.* **1987**, *137*, 107. (e) Duchowski, J. K.; Bocian, D. F. *J. Am. Chem. Soc.* **1990**, *112*, 3312.

Table 4. Experimental Determination of the Magnetic Moment in DCB[a]

compound	UV/nm	Γ/cm^{-1}	A/D[c]	μ	$[\theta]_1$	$[\theta]_2$	dif	sum	$B/D \times 10^4$	ϵ_m
ZnTNPc	684	539	2.965	-5.929	-229	191	-420	-39	8.975	150 400
(-1)[ZnTrNPc]$_2$	693[b]	1668	2.487	-4.974	-33	23	-56	-10	4.689	74 000
CoTNPc	681	1480	3.887	-7.775	-63	47	-110	-16	6.730	82 500
(-1)[CoTrNPc]$_2$	694[b]	3100	3.933	-7.866	-17	17	-34	0		52 800
H_2TNPc	709				-43.5				20.06	111 000
(-1)[H_2TrNPc]$_2$	700[b]				-50.05				33.76	75 900

[a] In order to obtain A/D values by Briat's method,[27] $[\theta]_1$ and $[\theta]_2$ in this table are expressed by molar ellipticity per unit gauss. Γ is the width at half-maximum absorption. dif = $[\theta]_1 - [\theta]_2$, sum = $[\theta]_1 + [\theta]_2$, and $A/D = -1.97\Gamma(\text{dif})/\epsilon_m$, while $B/D = -3.47(\text{sum}/\epsilon_m)$. Faraday A and B are being expressed by β·debye^2 and β·debye^2/cm^{-1}, respectively as in Stephens, P. J.; Suetaak, W.; Schatz, P. N. *J. Chem. Phys.* **1966**, *44*, 4592. [b] Average values of the two split Q peaks. [c] A/D values under a new definition (Piepho, S. B.; Schatz, P. N. *Group Theory in Spectroscopy*; John Wiley & Sons: New York, Chichester, 1983) are obtained by dividing these values by 2.

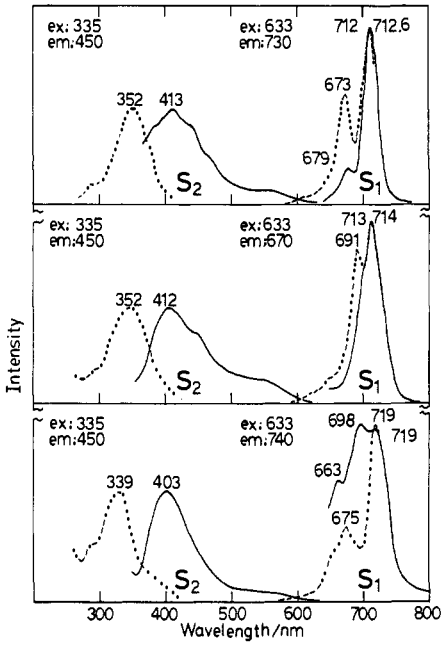

Figure 4. Fluorescence emission (solid lines) and excitation spectra (broken lines) of H_2TNPc (top), (-1)[H_2TrNPc]$_2$ (middle), and (-1)-[ZnTrNPc]$_2$ (bottom) in chloroform. In each species, there is no intensity relationship between the S_1 and S_2 emissions. Excitation wavelengths and emission wavelengths used to record excitation spectra are shown. The absorbance at the excitation wavelengths was always less than 0.05.

Table 5. Quantum Yields (ϕ_F) and Lifetimes (τ) of Several Phthalocyanines in Deaerated Chloroform at Room Temperature[a]

	S_1		S_2		
compound	ϕ_F	τ/ns	$\phi_F \times 10^4$	τ_1/ns (%)	τ_2/ns (%)
H_2TNPc	0.243	7.29	5.6	3.53 (50.1)	13.0 (49.9)
(-1)[H_2TrNPc]$_2$	0.037	4.26	8.7	5.00 (51.4)	17.2 (48.6)
ZnTNPc	0.246	3.94	14.8	1.63 (32.0)	12.5 (68.0)
(-1)[ZnTrNPc]$_2$	0.040	2.76	27.5	3.42 (20.7)	15.8 (79.3)

[a] Excitation wavelengths for S_1 and S_2 emissions were at 633 and 335 nm, respectively. Because of solution instability, ϕ_F values of S_2 emission were obtained using the first spectra recorded after deaeration.

to an intradimer charge-transfer band. However, in no case was there reported any band which corresponds to the 845-nm peak seen in this study.

Spectroelectrochemistry of the reduction of the (-1)[ZnTrNPc]$_2$ derivative is of particular interest since, to our knowledge, no reports on the spectroscopy of mixed-valence ring-reduced phthalocyanines have previously been made. Figure 5B shows the spectroscopic changes observed during stepwise reduction of (-1)[ZnTrNPc]$_2$ across the first three one-electron reduction couples, to form the mixed-valence (-1)[ZnTrNPc(-2)·ZnTrNPc(-3)]$^-$ species, the doubly ring-reduced (-1)[ZnTrNPc(-3)]$_2^{2-}$ species, and the second ring-reduced mixed-valence (-1)-[ZnTrNPc(-3)·ZnTrNPc(-4)]$^{3-}$ species, respectively. The changes in the Soret- and Q-band regions are not as marked as those seen during oxidation, the most notable effect being a pronounced narrowing of the Q band upon formation of the doubly ring-reduced (-1)[ZnPc(-3)]$_2^{2-}$ species. The Q-band width of this and the trianion is almost the same as that of monomeric ZnTNPc, suggesting that the negative charges in each Pc unit of the (-1)-Pc_2 act repulsively. More pronounced changes are seen in the near-IR band, whose intensity approximately doubles on formation of the first mixed-valence species, and then decreases again to the level of the neutral complex on formation of the second mixed-valence species. It is interesting to note the sensitivity of the near-IR band to the redox state of the molecule during both oxidation and reduction and that the largest changes in intensity of this band occur when the (-1)Pc_2 forms a mixed-valence species containing an odd number of electrons in the Pc ring system.

Although not shown, MCD spectra of the species in Figure 5A,B were also recorded. The intensity of the Q-band MCD of dicationic (-1)[ZnTrNPc]$_2$ is *ca.* one-fourth to one-fifth that of the neutral starting species, while the Faraday B term corresponding to the near-IR band disappears. The shapes of the spectra of the reduced forms are relatively similar to each other, except that the *pseudo* Faraday A term in the main Q band becomes sharper and its apparent intensity approximately doubles. In addition, a small B term emerges at *ca.* 760–770 nm.

The spectroscopic changes observed for (-1)[CoTrNPc]$_2$ during oxidation and reduction are already reported in our preliminary communication.[1] Stepwise oxidation across the first oxidation couple gives a spectrum typical of a phthalocyanine cation radical species, similar to that seen for (-1)[ZnTrNPc]$_2$, as described above, but with no clear spectroscopic evidence of any one-electron-oxidized intermediate. A similar phenomenon was observed in the case of Nap[CoTrNPc]$_2$ and Ant[CoTrNPc]$_2$.[9e] Although a clear near-IR band is not seen in the starting, neutral (-1)-[CoTrNPc]$_2$ species, there is a decrease in the absorbance of a shoulder at *ca.* 865 nm, while a new band appears at around 1000 nm. This implies that some conformational changes are occurring during oxidation, as in the case of the zinc derivative. In contrast, reduction of (-1)[CoTrNPc]$_2$ over the first and second reduction couples proceeds *via* two distinct one-electron steps, corresponding to the stepwise reduction of each of the cobalt atoms to Co^I. The formation of Co^I is indicated by the appearance of a new absorption in the region of 400–500 nm, associated with metal-to-ligand charge transfer (MLCT) from Co^I to the phthalocyanine ring.[11a,34] The spectrum of the mixed-valence Co^{II}–Co^I species obtained at -1.25 V is different from that of the fully reduced Co^I–Co^I species obtained at -1.50 V, in that it has a much weaker MLCT band. This implies that the added electron may be delocalized over the extended ring system. The spectrum of the fully reduced Co^I–Co^I species shows some unusual features not seen previously with Co^IPc species, having a split Q band and a new absorption peak at 825 nm. Polarization of the OTTLE negative to the couples at -1.69 and -1.93 V results in the formation of a ring-reduced species with a spectrum typical but red shifted compared to mononuclear ring-reduced [Co^ITNPc(-3)]$^{2-}$.[9b] The third and

(34) Stillman, M. J.; Thompson, A. J. *J. Chem. Soc., Faraday Trans. 2* **1974**, *70*, 790.

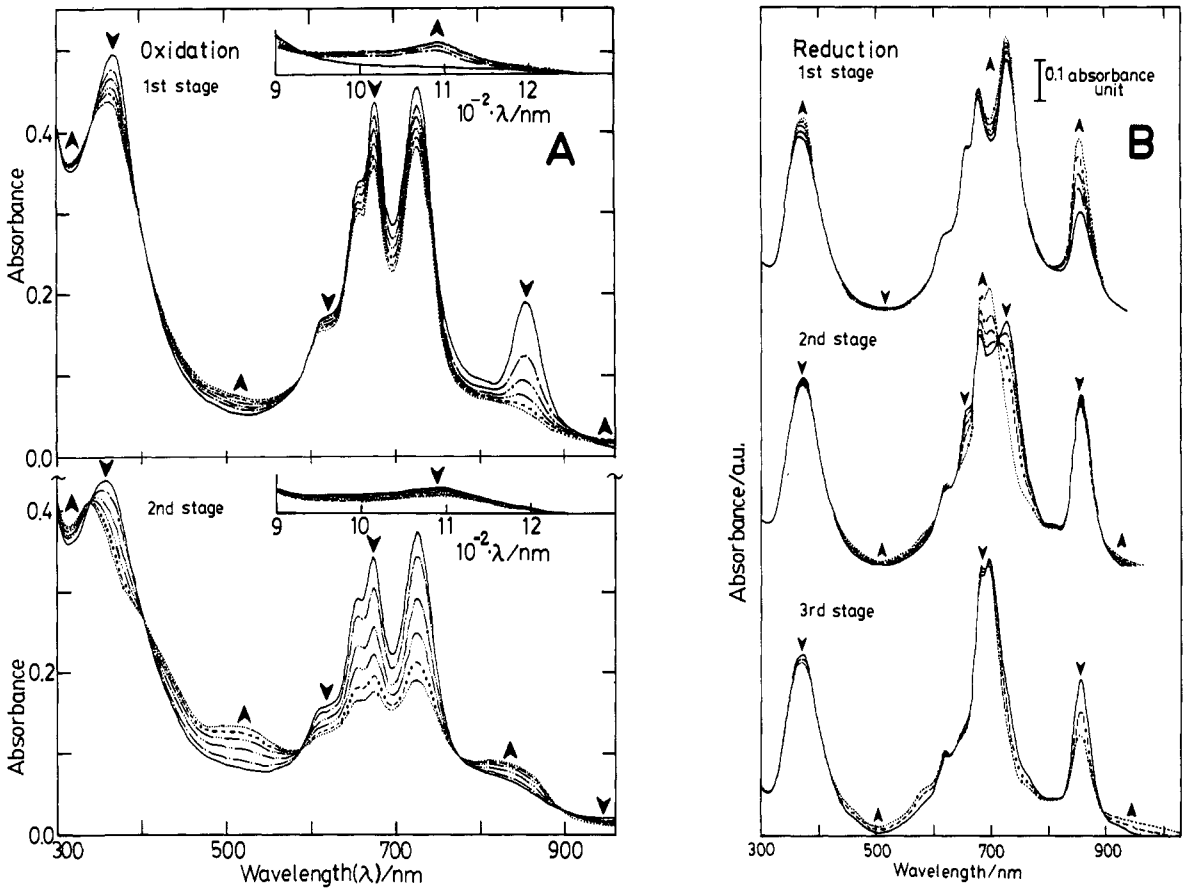

Figure 5. (A) Two-stage development of the electronic spectrum with time, during the oxidation of (−1)[ZnTrNPc]$_2$ at +0.50 V vs Fc$^+$/Fc in DCB (0.3 M TBAP) to a Zn^{II}–Zn^{II} ring-oxidized dication radical. [(−1)[ZnTrNPc]$_2$]/M = 1.72 × 10^{-4}. Cell path length/mm = 1.0. The directions of spectroscopic change are shown by the bold arrows. (B) Two-step three-stage development of the electronic spectrum with time, during the reduction of (−1)[ZnTrNPc]$_2$ in DCB containing 0.3 M TBAP to Zn^{II}–Zn^{II} ring-reduced mono-, di-, and trianion radicals. [(−1)[ZnTrNPc]$_2$]/M = 1.92 × 10^{-3}. Cell path length/mm = 0.45. The applied potentials used to obtain the monoanion, dianion, and trianion species were −1.6, −2.0, and −2.2 V vs Fc$^+$/Fc, respectively. The directions of spectroscopic change are shown by the bold arrows.

fourth reduction couples at −1.69 and −1.93 V thus appear to be the stepwise first ring reductions, while the couples at −2.04 and −2.20 V may be the second ring reductions.

MCD changes observed on electrolysis of (−1)[CoTrNPc]$_2$ were also recorded (not shown). The spectra show increased structure in the region of 400-550 nm with progressive reduction, and the superimposition of two positive Faraday *A* terms of Co^I–Co^I ring reduced dianionic species indicates that cobalt is in a low-spin d^7 state[34] and that the splitting of the two MLCT bands is *ca.* 2200 cm^{-1}.

(iv) **Molecular Orbital Calculations.** In order to enhance our interpretation of the spectra of the planar phthalocyanine dinucleates, we have performed molecular orbital calculations for the tetraanion of (−1)[H$_2$TrNPc]$_2$ (*i.e.* (−1)Pc$_2$) and the dianion of H$_2$TNPc (*i.e.* Pc) within the framework of the PPP method. The calculations reveal several noteworthy aspects which are useful in interpreting the absorption spectra. As detailed in previous publications,[35] in a one-electron description the phthalocyanine Q band corresponds to a transition from the highest occupied molecular orbital (HOMO) to the doubly degenerate, lowest unoccupied molecular orbital (LUMO), and the Soret band is associated with a transition from the second HOMO to the LUMO. For Pc, the present PPP calculations reveal these transitions to be at 662 and 332 nm, which is in good agreement with experiment (684 and 349 nm of ZnTNPc) and demonstrates

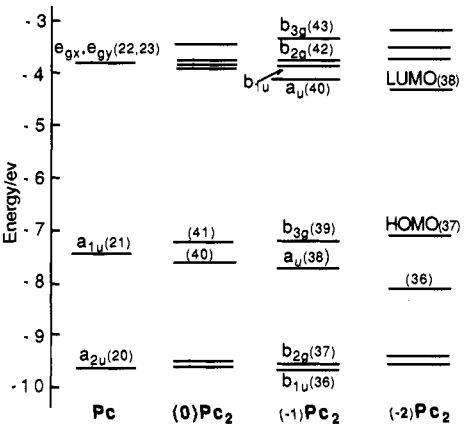

Figure 6. Partial molecular orbital energy diagram for (pyrrole proton-) deprotonated phthalocyanine and planar binuclear phthalocyanine macrocycles.

the reliability of the parametrization. Turning to the case of the planar binuclear phthalocyanines, the degenerate pair of orbitals comprising the lowest unoccupied level in mononuclear Pc split into two levels, and therefore two split Q bands are calculated, but at longer wavelength: 783 and 685 for (0)Pc$_2$; 847 and 682 nm for (−1)Pc$_2$; and 970 and 701 nm for (−2)Pc$_2$. This relationship is shown in Figure 6 with data given in Table 6. The calculated values lie in the correct direction, but fall somewhat toward longer wavelength compared to the experimental values (*e.g.* 715 and 672 nm for (−1)[ZnTrNPc]$_2$). In addition, the values indicate that the Q-band splitting increases the smaller the size of the

(35) (a) Gouterman, M.; Wagniere, G. H. *J. Mol. Spectrosc.* **1963**, *11*, 108. (b) Dale, B. W. *Trans. Faraday Soc.* **1969**, *65*, 331. (c) Hendriksson, A.; Roos, B.; Sundbom, M. *Theor. Chim. Acta* **1972**, *27*, 303. (d) Lee, L. K.; Sabelli, N. H.; LeBreton, P. R. *J. Phys. Chem.* **1982**, *86*, 3926. (e) Schaffer, A. M.; Gouterman, M. *Theor. Chim. Acta* **1972**, *25*, 62.

Table 6. Calculated Transition Energies, Oscillator Strengths (f), and Configurations for Deprotonated Mononuclear Pc, Planar Binuclear (–1)Pc_2, and Related Systems[a]

energy	f	configurations[b]
		Pc
1.8736	0.8435	0.9354 (21, 22), –0.3481 (20, 23)
1.8736	0.8435	–0.9354 (21, 23), –0.3481 (20, 22)
3.7347	2.1941	0.8194 (20, 23), +0.3443 (13, 23), +0.3259 (21, 22)
3.7347	2.1941	–0.8194 (20, 22), –0.3443 (13, 22), +0.3259 (21, 22)
		(0)Pc_2
1.5847	2.3325	0.8905 (41, 42), +0.3666 (40, 45)
1.8100	1.6193	–0.8116 (41, 43), –0.4784 (40, 44), +0.2561 (38, 42)
3.4818	2.3141	0.6315 (39, 42), +0.4639 (38, 43), +0.4158 (37, 44), –0.3208 (40, 45)
3.7738	3.8619	0.6300 (38, 42), +0.4375 (37, 45), +0.3572 (39, 43)
3.8133	1.2395	0.6853 (39, 42), –0.4324 (38, 43), –0.3105 (37, 44)
3.8479	0.4248	–0.8320 (39, 43)
		(–1)Pc_2
1.4645	2.2117	0.9371 (39, 40), +0.2539 (38, 43)
1.8173	1.3313	–0.8438 (39, 41), –0.3558 (37, 40), +0.2773 (37, 40)
3.6245	3.3430	–0.6445 (37, 41), –0.5011 (36, 42), +0.3805 (38, 43)
3.7214	4.1807	0.7012 (37, 40), +0.3653 (36, 43), –0.3317 (24, 40)
		(–2)Pc_2
1.2790	2.1895	0.9606 (37, 38)
1.7695	1.0143	–0.9106 (37, 39), –0.3222 (35, 38)
3.2290	0.6673	–0.6673 (36, 41), –0.5775 (37, 42)
3.5112	3.7540	–0.8149 (35, 38), +0.3629 (36, 40), +0.25 (37, 39)
3.6316	2.8512	0.7189 (35, 39), +0.4452 (36, 41), +0.3632 (34, 40)

[a] Excited states with energy less than 3.9 eV and f greater than 0.3 are shown. [b] (a,b) represents a configuration a → b; coefficients greater than 0.3 are shown except in a few cases of the Q and Soret bands.

shared aromatic unit, being 3956, 2845, and 1817 cm^{-1} for (–2)-Pc_2, (–1)Pc_2, and (0)Pc_2, respectively. Concerning the intensity of the two split Q bands, the calculated intensity (oscillator strength) to lower energy always appears larger than that to higher energy, in agreement with experiment (compare for example the two peaks at 715 and 672 nm of (–1)[ZnTrNPc]$_2$). Moreover, as shown by the configurations in Table 6, the calculations predict for all the planar binucleates, in the one-electron description, that the Q band to lower energy corresponds to a transition from the HOMO to the first LUMO while that to higher energy is associated with a transition from the HOMO to the second LUMO. Relatively analogous predictions, which, however, differ in a few aspects, are obtained in the Soret-band region also. Although it is generally accepted[35] that the Soret bands of mononuclear Pc are less pure than the Q band and that they are comprised mainly of a_{2u} (the second HOMO) to e_g (LUMO) excitation under D_{4h} symmetry, the results for the binuclear species can be reasonably interpreted if we assume that the second HOMO level in mononuclear Pc splits into two levels. In other words, similarly to the Q bands, the Soret bands of the binucleates lie at two different wavelengths. However, there is no clear linear relationship between the splitting energy and the size of the shared aromatic molecule (971, 782, and 2355 cm^{-1} for (–2)Pc_2, (–1)-Pc_2, and (0)Pc_2, respectively). There is a tendency that, similar to the case of the Q band, the calculated Soret band appears at longer wavelength compared to the monomeric Soret band. This is in fact observed experimentally for the zinc complexes, but not as clearly in the cobalt complexes. Further, as can be conjectured from the values of the configurations in Table 6, transitions from the third and/or fourth HOMOs to the first and/or second LUMOs contribute substantially to the Soret band. Another notable point in Figure 6 is the anticipation that, although both the a_{1u} and a_{2u} orbitals in D_{4h} phthalocyanine are split in the D_{2h}-type binuclear phthalocyanines, the splitting of the former is much larger.

In Figure 7, we show the four HOMOs and four LUMOs of (–1)Pc_2, together with the two HOMOs and two degenerate LUMOs of Pc. It is interesting to note that the eight frontier

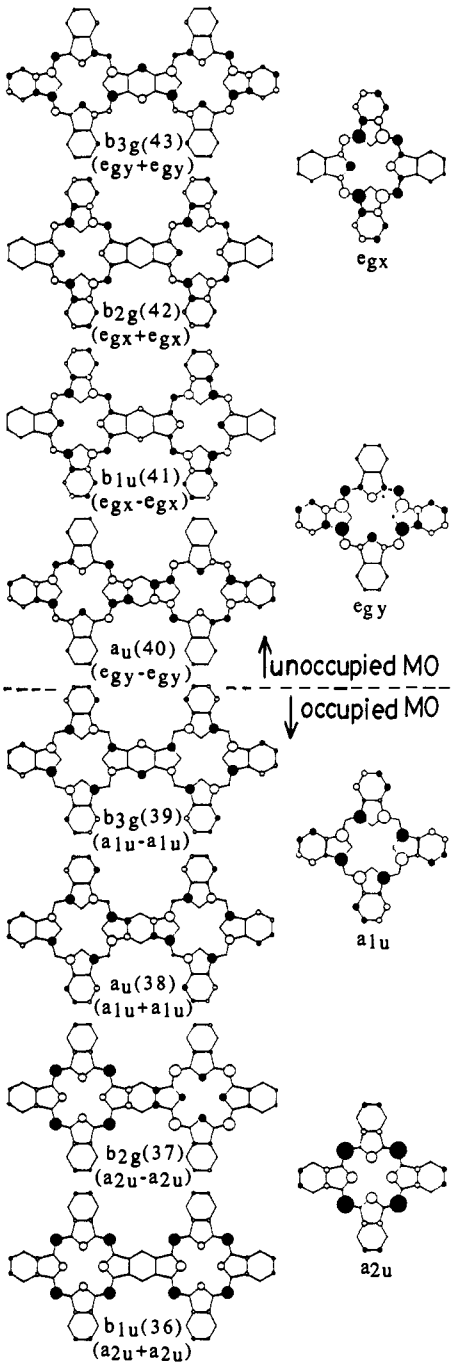

Figure 7. Eight frontier orbitals of (–1)Pc_2 and four frontier orbitals of Pc. Note that the e_{gx} and e_{gy} orbitals are degenerate. The parentheses under each MO of (–1)Pc_2 indicate the expression of MO by the notation in D_{4h} symmetry which is used for Pc.

orbitals of (–1)Pc_2 can be expressed by a linear combination of the MOs of mononuclear Pc (this is shown below each MO). The first and second HOMOs can be expressed only by the use of two a_{1u} orbitals, while the third and fourth HOMOs can be described using two a_{2u} orbitals in D_{4h} symmetry. Similarly, the four LUMOs are expressed only by the use of e_{gx} and e_{gy} orbitals.

The results described above on the MO calculations of binuclear phthalocyanines are not contradictory to the argument in section ii that two relatively independent phthalocyanine chromophores are interacting with each other in the planar binuclear phthalocyanines of the present study. However, no suggestion is made on the origin of the weak near-IR band appearing to the red of the Q band, since completely planar binuclear structures were assumed in the calculations. One referee pointed out the possibility of the occurrence of an intramolecular charge-transfer band and

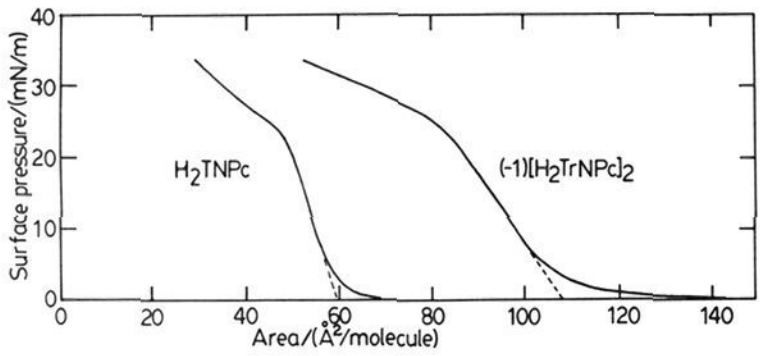

Figure 8. Surface pressure vs area per molecule isotherms for H_2TNPc and $(-1)[H_2TrNPc]_2$ on triply distilled water at 10 °C.

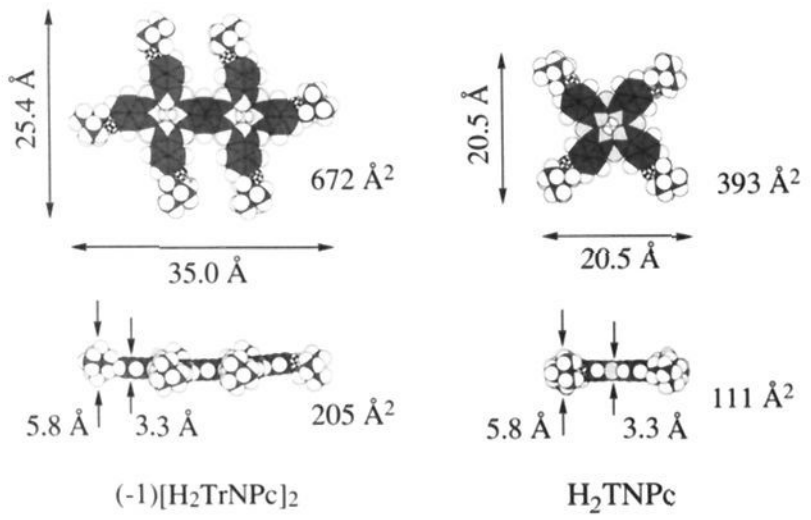

Figure 9. Molecular dimensions of H_2TNPc and $(-1)[H_2TrNPc]_2$ estimated by the CPK molecular model.

asked whether it could be detected by ESR. However, no such evidence was obtained in measurements down to 11 K in deaerated toluene.

(v) Monolayers and Built-Up Mutilayer LB Films of H_2TNPc and $(-1)[H_2TrNPc]_2$. Over the past 10 years, a number of reports[36,37] have appeared on the fabrication, characterization, and application of Langmuir–Blodgett films using soluble phthalocyanines, in the hope that a highly ordered structure may improve their diverse functions. While mononuclear phthalocyanine derivatives have been used most extensively, a few reports on the LB behavior of dimers[36d,e,g,37a] and oligomers[36f,37a] have begun to appear recently. Here, we describe the monolayer and LB film behavior of $(-1)[H_2TrNPc]_2$, together with that of H_2TNPc for comparison.

Figure 8 shows the surface pressure versus area isotherms at 10 °C for monolayers of H_2TNPc and $(-1)[H_2TrNPc]_2$. Surface pressures begin to develop at a molecular area of *ca.* 70 Å² for H_2TNPc and 140 Å² for the binuclear complex, and the films become rigid in the range 45–55 Å² and 80–100 Å², respectively. If the molecular size is taken into account, the compressibility is approximately the same for the two compounds. Collapse of the films is observed at a relatively low pressure of around 24 mN m^{-1} for both compounds. The limiting areas per molecules are 60 Å² for H_2TNPc and 108 Å² for $(-1)[H_2TrNPc]_2$. If we accept the molecular dimensions shown in Figure 9, which were estimated by the CPK molecular model, these values are considerably smaller than those occupied in an edge-on stack (111 and 205 Å², respectively). This indicates that both compounds are in the form of a slipped stack, with the phthalocyanine plane parallel to the air–water interface[36a] (see Figure 10). Since H_2TNPc occupies a minimum area of about 393 Å² in a plane, division of 393 by 47 (the area at 24 mN m^{-1} where the monolayer collapses) indicates a stack of *ca.* 8.4 molecules. Similarly, a stack of 8.2 molecules is obtained for $(-1)[H_2TrNPc]_2$.

From X-ray studies on built-up LB films of $(-1)[H_2TrNPc]_2$ formed by 20 dippings, the thickness of the monolayer was obtained from the $2\theta = 4.0°$ reflection and the shortest spacing for a coplanar Pc ring appeared at $2\theta = 22.4°$ with a line breadth of about 4°. Assuming that the binuclear Pc plane has edges of 25 and 35 Å, the mean tilt angle (δ) of the molecular plane to the normal of the plane of the substrate is evaluated as 28° (for 25 Å) or 51° (for 35 Å) from the thickness per monolayer in the built-up LB film. According to these values, the molecular plane appears to take an edge-on configuration on the quartz plate in the form of face-to-face stacking with a tilt angle (Figure 10).

Figure 11 shows the absorption spectra of built-up LB films and spin-coated nonoriented films of H_2TNPc and $(-1)[H_2TrNPc]_2$ on quartz plates, together with those taken in chloroform solution. Compared with the monomeric solution spectra, the Q bands of the spin-coated and LB films are broad and shifted to shorter wavelength, indicating that the phthalocyanines are in an aggregated form having a cofacial arrangement.[9d-f,10,28,38] In this case, the assembling number of phthalocyanine stacks, N, can be evaluated simply and semiempirically by use of the following equation.[36b,c]

$$N = \Delta E(N\rightarrow\infty)/\{\Delta E(N\rightarrow\infty) - \Delta E(N)\} \qquad (2)$$

where $\Delta E(N)$ is the exciton shift for phthalocyanine stacks with an assembling number N, and $\Delta E(N\rightarrow\infty)$ is the exciton shift for an infinite phthalocyanine stack. From Figure 11, the value of $\Delta E(N)$ for H_2TNPc is approximately 1300 cm^{-1}, and since $\Delta E(N\rightarrow\infty)$ is generally around 1500–1700 cm^{-1} for mononuclear phthalocyanines,[36b,c] the value of N for H_2TNPc is calculated to be about 4–8. The $\Delta E(N\rightarrow\infty)$ value for a planar binuclear molecule is not known; however, judging from the smaller blue-shift compared with the H_2TNPc system, the assembling number of $(-1)[H_2TrNPc]_2$ does not appear to be large.

It is instructive to use polarized light to help identify the preferred orientation of the molecules in the built-up LB films. Figure 12 (top) compares the angular dependence of the absorption intensity at several wavelengths for the built-up LB films and spin-coated nonoriented films (θ is the angle between the incident light and substrate normal). Since it is necessary to take into account the reflection of incident light at the surface of the films,[39] the absorbances of the LB films were corrected by subtracting the absorbances of the spin-coated films (Figure 12, bottom). The absorbance in the Soret region is seen to change more sensitively than that of the Q-band region for both the mononuclear and binuclear complexes, and with the exception of the $(-1)[H_2TrNPc]_2$ 700-nm absorption, minima are recorded at $\theta = 0°$. In order to interpret these results, we must consider the effect on the absorption spectrum of the relationship between the incident angle (θ) of the polarized light and the orientation (θ') of the transition moment of the chromophore on the substrate, as shown in Figure 13A. The absorption intensity is maximum when the electric vector of the incident light (**E**) is coupled most strongly with the transition moment (**M**) of the chromophore, while inversely, it becomes 0 when there is no coupling. This situation can be easily understood by considering the two extreme cases in Figure 13A. If, for example, both θ and θ' are 0, **E** and **M** will not couple since they are perpendicular to each other, and hence the absorption intensity becomes 0. Conversely, if $\theta' = 0°$ and $\theta = 90°$, the coupling of **E** and **M** is maximum, since they are now parallel, and as a result, the strongest absorption is obtained. In Figure 13B, we show the detailed incident-light-angle depen-

(36) (a) Barger, W. R.; Snow, A. W.; Wohltjen, H.; Jarvis, N. *Thin Solid Films* **1985**, *133*, 197. (b) Fujiki, M.; Tabei, H.; Imamura, S. *Jpn. J. Appl. Phys.* **1987**, *26*, 1224. (c) Fujiki, M.; Tabei, H.; Kurihara, T. *J. Phys. Chem.* **1988**, *92*, 1281; *Langmuir* **1988**, *4*, 1123. (d) Gupta, S. K.; Hann, R. A.; Twigg, M. V. *Thin Solid Films* **1989**, *179*, 343. (e) Petty, M.; Lovett, D. R.; O'Connor, J. M.; Silver, J. *Ibid.* **1989**, *95*, 6979. (f) Sauer, T.; Arndt, T.; Bachelder, D. N.; Kalachev, A. A.; Wegner, G. *Ibid.* **1990**, *187*, 357. (g) Liu, Y.; Shigehara, K.; Yamada, A. *J. Am. Chem. Soc.* **1991**, *113*, 440.

(37) (a) Kim, J.-H.; Cottom, T. M.; Uphaus, R. A.; Leznoff, C. C. *Thin Solid Films* **1988**, *159*, 141. (b) Itoh, H.; Koyama, T.; Hanabusa, K.; Masuda, E.; Shirai, H.; Hayakawa, T. *J. Chem. Soc., Dalton Trans.* **1989**, 1543.

(38) (a) Sharp, J. H.; Lardon, M. *J. Phys. Chem.* **1968**, *72*, 3230. (b) Sharp, J. H.; Abcowitz, M. *J. Phys. Chem.* **1973**, *77*, 477.

(39) Suzuki, T. Thesis, Shinshu University, 1991.

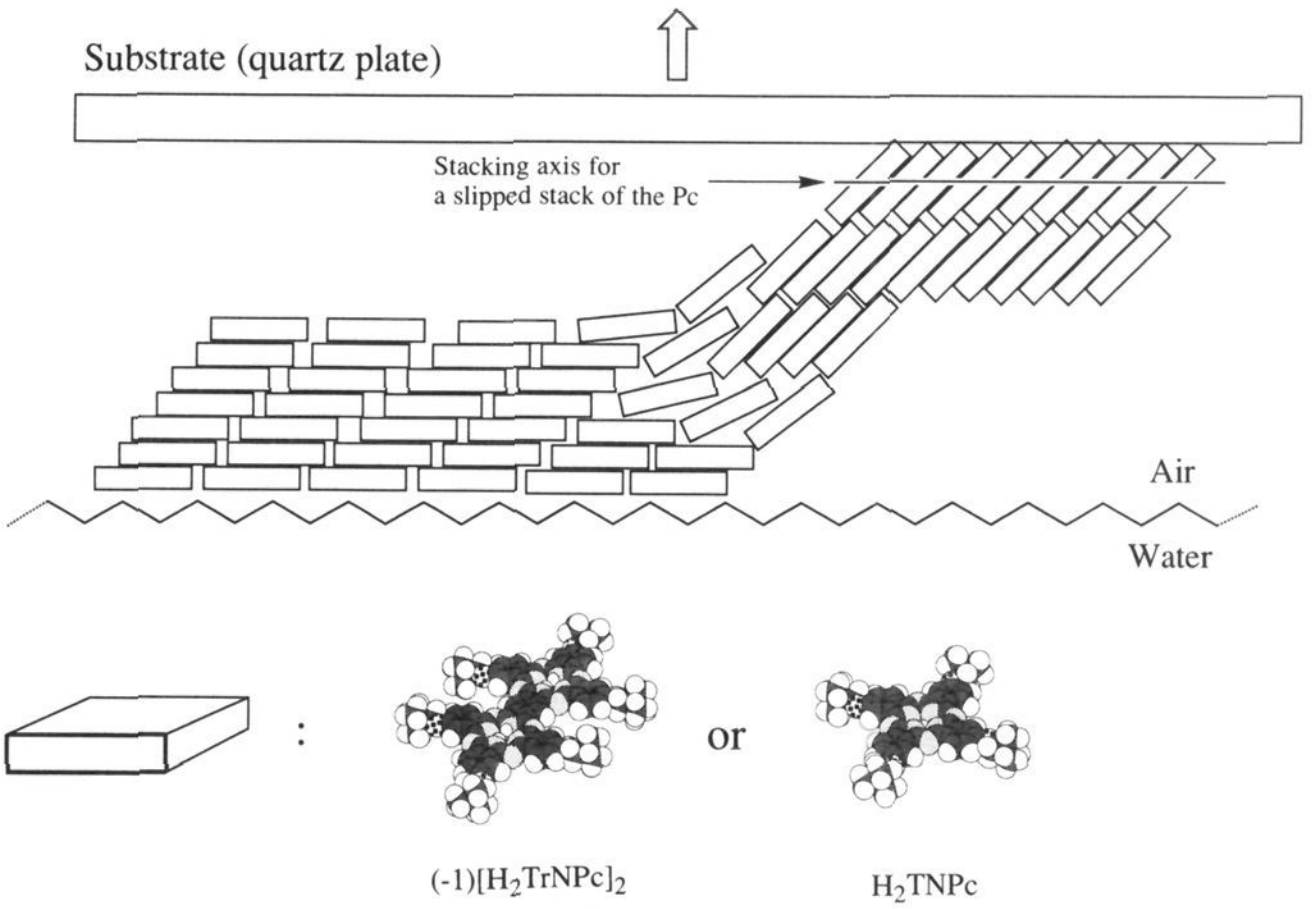

Figure 10. Model for the transfer of the Pc LB film from an air–water interface to a substrate surface.

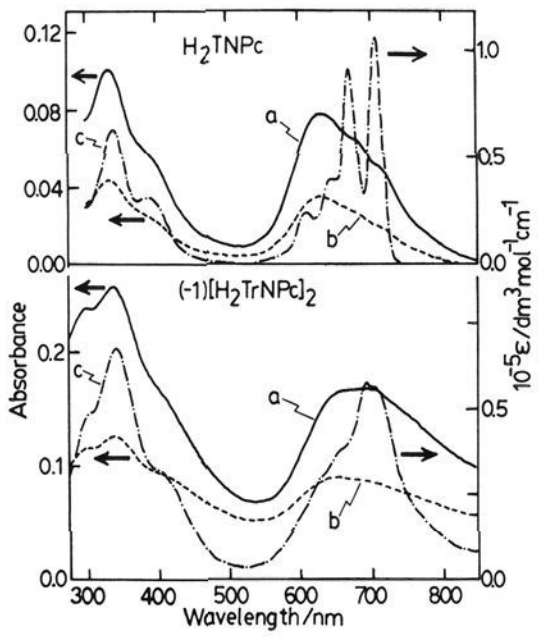

Figure 11. Electronic absorption spectra of H_2TNPc (top) and (–1)-[H_2TrNPc]$_2$ (bottom) LB films (curves a), spin-cast films (curves b), and chloroform solution (curves c).

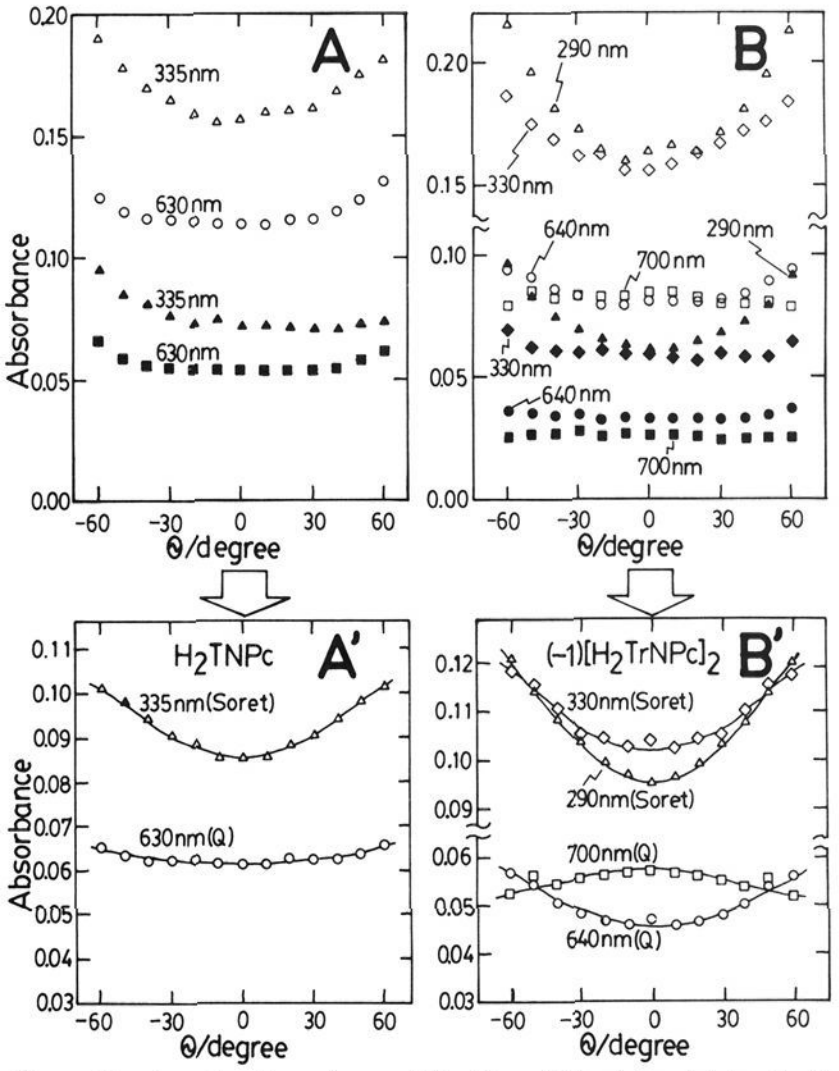

Figure 12. Angular dependence of the Q- and Soret-band intensity for (A) H_2TNPc and (B) (–1)[H_2TrNPc]$_2$ LB films deposited on hydrophobic quartz substrates by the horizontal lifting method (20× dipping at 16 mN/m) (empty symbols) and their nonoriented films (filled symbols). A′ and B′ are corrected data, obtained by subtracting the nonoriented film values from the LB film data.

dence of the theoretical absorption intensity at various tilt angles, θ'. This figure predicts that the relative absorption intensity minimizes at $\theta = 0°$ when the transition moment is tilted by less than 54.7°, producing a "dip-type" curve. In contrast, when θ' is more than 54.7°, the angular dependent curve having a "hip-type" shape is produced. From this, we can deduce that θ' in our H_2TNPc LB films is less than 54.7°. The difference between the angular dependence of the absorption intensities at 335 and 630 nm seen for H_2TNPc (Figure 12, bottom left) may reflect the different nature of the Soret and Q bands in phthalocyanines. According to a study on phthalocyanine crystals,[40] the transition moment of the Q band lies in the plane of the phthalocyanine ring, but that of the Soret band is mixed with a component lying perpendicular to the phthalocyanine plane due to pyrrole n–π^* transitions.[35,41] If, for example, the phthalocyanine molecules have a slipped-stack form with the stacking axis parallel to the substrate surface, and if the phthalocyanine plane is tilted at an angle of 45° to the surface ($\theta' = 90 - 45 = 45°$), the transition moments both in-plane and normal to the plane will interact with **E** in such a manner that the absorption intensity–incident light angle relationship shows a "dip-type" curve. In this case, the depth of the dip may be larger for the Soret band than for the Q band, since for the Soret band the coupling between **E** and **M** with direction normal to the phthalocyanine plane is added to the in-plane coupling. In contrast, for the Q band, a "dip-type"

(40) Lyons, L. E.; Walsh, J. R.; White, J. W. *J. Chem. Soc.* **1960**, 167.
(41) VanCott, T. C.; Janna, L. R.; Misener, G. C.; Williamson, B. E.; Schrimpf, A. E.; Boyle, M. E.; Schatz, P. N. *J. Phys. Chem.* **1989**, *93*, 2999.

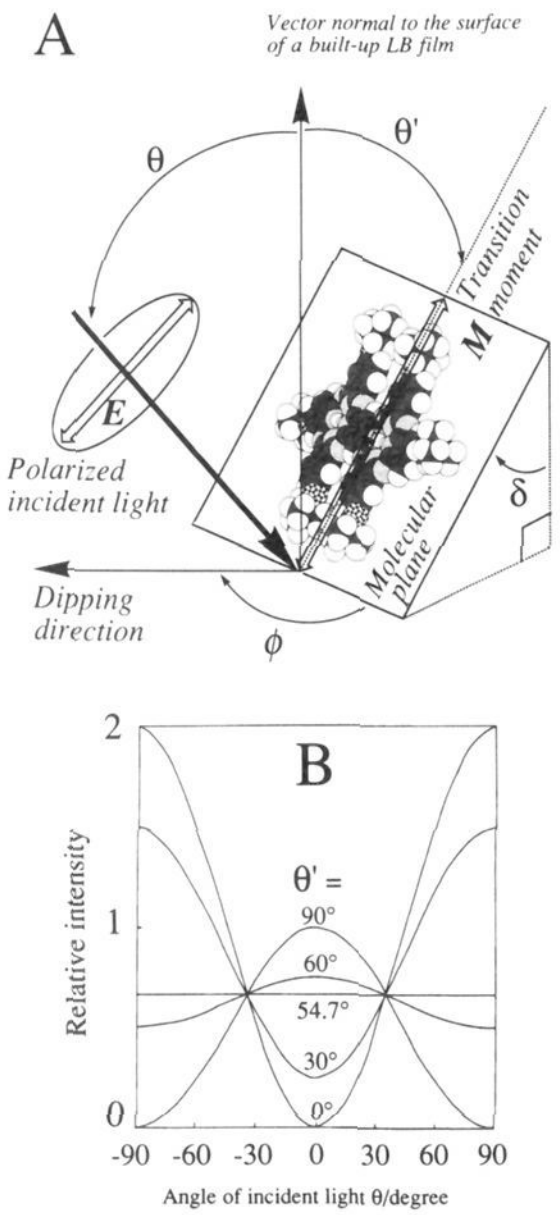

Figure 13. (A) Relationship between the direction of the incident polarized light and the chromophore transition moment. (B) Angular dependence of the theoretical absorption intensity calculated for a uniaxially orientated system at various tilt angles, θ'.

angular dependence of the absorption intensity is produced only by coupling between **E** and **M** in the plane of the phthalocyanine ring.

The situation in the case of the LB film of $(-1)[H_2TrNPc]_2$ (Figure 12, bottom right) appears to be more complex, but may be explained by assuming the existence of two kinds of structure, as follows. The Q band at 640 nm can be reasonably ascribed to a cofacial type of self-assembled structure, and the angular dependence of absorption intensity shows a "dip-type" curve at 640 nm and in the Soret region. Then, from Figure 13B, it is deduced that the phthalocyanine plane in $(-1)[H_2TrNPc]_2$ films is tilted from the substrate normal by less than 54.7°. Although the angular dependence of absorbance at 700 nm shows a "hip-type" curve, this appears to originate from monomeric $(-1)[H_2TrNPc]_2$, since 700 nm is the position of the Q band of monomeric $(-1)[H_2.TrNPc]_2$ (Table 1 and Figure 11). This implies from Figure 13B that the monomeric $(-1)[H_2TrNPc]_2$ molecule tilts by more than 54.7° from the axis perpendicular to the substrate, and it may plausibly be lying almost flat on the substrate surface. The existence of more than one structure in the $(-1)[H_2TrNPc]_2$ system is also suggested by comparison of the absorption spectra of the LB films of H_2TNPc and $(-1)[H_2TrNPc]_2$ (Figure 11, solid lines). Compared with the large blue-shift of the Q band in the LB film from that in solution in the H_2TNPc system, the shift for the $(-1)[H_2TrNPc]_2$ system is much smaller, indicating that the average stacking number is less than in the H_2TNPc system. Since the stacking number in the H_2TNPc LB film is estimated to be 4–8, it is not unreasonable to conclude that some of the $(-1)[H_2TrNPc]_2$ molecules may exist as monomers.

(vi) Concluding Comments. Metal-free, dizinc, and dicobalt planar binuclear phthalocyanines have been extensively studied using various methods for the first time in the phthalocyanine and porphyrin family. As in the case of the cofacial-type phthalocyanines,[9g,h,10,11] many phenomena have been rationalized as being due to the interaction between two almost independent chromophores. Thus, the simple absorption peaks of mononuclear control molecules split into two peaks each in the binucleates, and the weak Faraday *A*-term-like MCD curves in the Q band of the binuclear complexes are interpreted as the sum of two closely-located Faraday *A* terms. The emergence of a band at lower energy than the Q band indicates, on the basis of previous knowledge of the absorption spectra of dimers,[25,26] that the two phthalocyanine units in the binuclear molecule have a slightly bent conformation about the common benzene ring. Since the intensity of this near-IR band changes with progressive oxidation or reduction, it is suggested that the intramolecular angle connecting the two phthalocyanine units varies with the redox state of the macrocycle. All redox couples seen in the mononuclear control molecules split into two in the binuclear complexes, but the splitting of the first oxidation couple is not as clear as that of the reduction couples.

Fluorescence emission from S_1 and S_2 states is observed for metal-free and zinc complexes. The quantum yields and lifetimes of the S_1 emission of the binuclear complexes are smaller than for the corresponding mononuclears, as has been observed previously for dimeric porphyrins.[7b,d] However, the nature of the S_2 emission differs from that of the S_1 emission in several aspects. Two components are always required in the analysis of the lifetime, one of which has a very long lifetime of 12–18 ns. In addition, the S_2 quantum yields of the binuclear complexes are larger than those of the mononuclear compounds.

Molecular orbital calculations have helped to elucidate the nature of the electronic absorption spectra. Both the Q and Soret bands split into two as if the a_{1u}, a_{2u}, and two e_g orbitals under D_{4h} symmetry split into two (the former two) or four (the latter one) orbitals. The calculations also show that the smaller the size of the shared aromatic linkage between the two phthalocyanine units, the larger will be the splitting of the Q band.

Monolayers of H_2TNPc and $(-1)[H_2TrNPc]_2$ were prepared at an air–water interface. Analysis of surface pressure–area isotherms indicates that in both compounds the molecules on the water surface are in a slipped-stack arrangement, with the molecular plane parallel to the air–water interface (Figure 10). Built-up LB films of these compounds have been prepared by the horizontal lifting method. The assembling numbers are evaluated as being *ca.* 4–8 for H_2TNPc and less than this for $(-1)[H_2TrNPc]_2$. From the angular dependence of the absorption intensity in these films, it appears that the self-assembled molecules are not completely disordered but may have a slipped-stack conformation, with the stacking axis parallel to the surface of the substrate (Figure 10). The evidence also implies that in the case of the binuclear complex there may be a second structural component consisting of monomeric-type molecules orientated approximately flat on the substrate surface.

Acknowledgment. We are indebted to Dr. H. Konami for his help in MO calculations.